Consolidation – creep modeling of pilot data on deposition of flocculated fluid fine tailings

Narges Gheisari, Shunchao Qi, Paul Simms
Department of Civil and Environmental Engineering, Carleton University, Ottawa, Ontario, Canada

ABSTRACT
Pilot studies of flocculated fluid fine tailings (fFFT) deposits are modeled using coupled large strain consolidation – creep formulations embedded in the UNSATCON software. The creep formulations employed are based on theory developed by Vermeer, a hypothesis B type model that implies a strain rate dependency on the location of the compressibility curve, and Yin and Graham model that has been formulated using the concepts of equivalent time. The pilots comprised deposits of tailings placed in 13 m tall x 2.75 m wide caissons. Here we present comparisons of data from tailings flocculated with a conventional anionic polymer. Simulations are presented for large strain consolidation only, as well as two different models to simulate creep – consolidation, using reasonable ranges in the k-e function and the creep parameters. The use of a creep model improves fits to all measured properties (settlement and excess pore-water pressure), compared to the consolidation only results, though agreement in still not perfect. Using different groups of plausible parameters sets, the model was then used to extrapolate to full scale behavior. In general, use of creep model results in relatively small (~10%) increase in the overall settlement of the deposits, but a marked decrease in the rate of pore-water pressure dissipation. The significance of these results to implantation for full scale deposits are discussed, as are areas of uncertainty requiring further attention.

RÉSUMÉ
Les études pilotes sur les dépôts de résidus fins fluides floculés (fFFT) sont modélisées à l'aide de formulations couplées de consolidation à grande déformation - fluage intégrées au logiciel UNSATCON. La formulation de fluage utilisée est basée sur la théorie développée par Vermeer, un modèle de type hypothèse B qui implique une dépendance de la vitesse de déformation sur l'emplacement de la courbe de compressibilité. Les pilotes comprenaient des dépôts de résidus placés dans des caissons de 13 m de hauteur x 2,75 m de largeur. Nous présentons ici des comparaisons de données provenant de résidus floculés avec un polymère anionique conventionnel. Les simulations sont présentées uniquement pour la consolidation à grande déformation, ainsi que pour la consolidation par fluage, en utilisant des plages raisonnables dans la fonction k-e et les paramètres de fluage. L'utilisation d'un modèle de fluage améliore l'ajustement à toutes les propriétés mesurées (profils de profondeur et de tassement de la densité et de la pression interstitielle), par rapport aux seuls résultats de consolidation, bien que l'accord ne soit toujours pas parfait. En utilisant différents groupes d'ensembles de paramètres plausibles, le modèle a ensuite été utilisé pour extrapoler à un comportement à pleine échelle. En général, l'utilisation du modèle de fluage entraîne une augmentation relativement faible (~10%) du tassement global des dépôts, mais une diminution marquée du taux de dissipation de la pression interstitielle. L'importance de ces résultats pour l'implantation de gisements à grande échelle est discutée, tout comme les zones d'incertitude nécessitant une attention particulière.

1 INTRODUCTION

The extraction of bitumen from surface mined ore has produced large volumes (~ 300 km^2, with dam heights exceeding 100 m) of clayey tailings that have poor consolidation properties. Current regulations dictate the tailings must be rendered “ready to reclaim” within 10 years after end of mine life. Some operators believe that “ready to reclaim” implies that the tailings have strength enough to be stable in gently sloped deposits, of similar topography to the surrounding boreal uplands. Simple slope stability calculations suggest that this would require an undrained strength of 20 kPa (McKenna et al.2016), which in turn requires the tailings to reach their plastic limit, about 40%.

Despite dewatering technologies that can reduce water content of tailings; consolidation is still the dominant dewatering mechanism. The consolidation of soft soil deposits in many geotechnical engineering practices, such

as the various types of tailings, is often studied analytically or numerically based on Gibson's one-dimensional finite strain consolidation theory for saturated soils (Gibson et al. 1967). However, even after polymer induced flocculation treatments, the hydraulic conductivity of the tailings remains relatively low, and substantial settlement is expected over periods of years to decades. In this time scale, time dependent effects, such as creep and aging become important long-term deformations, as such time dependent behaviour has been reported in polymer amended FFT, by Salam et al. (2017) who ran several short (10 cm high) column tests on fFFT. So, this behaviour could have significant influence on the dewatering, consolidation and strength gain of tailings deposits, and therefore should be considered in large strain consolidation analysis, and large strain consolidation analysis is insufficient to predict dewatering or volume change in soft deposits (Sills 1999, Jeeravipoolvarn 2009).

Several kinds of numerical analysis have been developed that incorporate time-dependent behavior into consolidation (Hinchberger and Rowe 1998, Yin and Graham 1994, Bartholomeeusen 2002). Models based on empirical, rheological, and general stress-strain-time concepts have been proposed which elasto-visco-plastic models combine inviscid elastic and time-dependent plastic behavior (Vermeer & Neher, 1999; Yin & Graham, 1999). A comprehensive review of creep models can be found in Liingaard et al. (2004).

In this paper, in order to investigate dewatering behavior of oil sands tailing, two elasto-visco-plastic models (EVP) that proposed by Yin and Graham (1994, 1999), and also Vermeer and his co-workers (Stolle et al., 1997; Vermeer et al., 1998) are selected to simulate consolidation of flocculated fluid fine tailings (fFFT) deposits in the pilot study. For this purpose, the large strain consolidation software UNSATCON (Qi et al. 2017, 2019) is used for numerical modeling and the results are presented and discussed. Moreover, to investigate the results of creep-consolidation for full scale deposits, two hypothetical cases with different input parameters were conducted, based on plausible parameters estimated using the pilot scale data.

2 NUMERICAL MODELLING APPROACH

UNSATCON is a research code that simulates large strain-consolidation of saturated and unsaturated soft soil deposits while considering stress/desiccation history and hydraulic hysteresis (Qi et al. 2019, Qi et al. 2017 a, b). In other words, it can simulate the tailings' initial consolidation/dewatering process induced by self-weight and post-settling consolidation/dewatering process induced by evaporation in a coherent manner. It includes a number of new important features/capabilities: (1) mass conservation is strictly ensured in the algorithm, which is an important consideration in evaluating the effectiveness of various method to dewater tailings; (2) it can deal with complicated hydraulic exchange between atmosphere and tailing across the top moving surface; (3) it ensures a smooth state transition modeling (soil's state switches between saturated and unsaturated states). Lately, the UNSATCON code was adapted for creep-consolidation modeling compatible with large strain conditions (Qi et al. 2017). In this study, two elasto-visco-plastic models are compared to observed pilot data to evaluate the potential and limitations of these models to simulate the real behavior of dewatering in oil sands tailings.

3 DESCRIPTION OF THE PILOT STUDY

The pilot study involved deposition and monitoring of different types of treated fluid fine oil sands tailings (FFT) deposited into a steel casing approximately 2.75 m in diameter and 13 m in height. Monitoring data including solid content, effective stress, excess pore water pressure for different depths of tailing, and the heights of mudline. Monitoring data in this paper were recorded over a period of 3 years.

4 MATERIAL PARAMETERS

4.1 Permeability function

In this study, the power relationship is adopted and written as:

$$k = H_1 \times e^{H_2} \quad [1]$$

Where k is the saturated permeability. H_1, H_2 are two constants determined from experiments. In this study, as the authors were not provided with initial estimates of these properties three different methods were adopted to determine the hydraulic conductivity function:

4.1.1 Method1: Estimation from Atterberg Limits or the compressibility function

Recently, Babaolgu and Simms (2020, 2018) suggested equations for slurry permeability, that require only 1 measurement of hydraulic conductivity at high void ratio or low effective stress. This value of hydraulic conductivity can be obtained using Pane and Schifman's (1997) method, which requires the initial linear slope of the settlement curve, and the solids concentration at the tailings- water interface, void ratio and the velocity of water-tailing interface. Therefore, hydraulic conductivity can be estimated using the following equations:

$$k = k_{\text{measured at } e_0} \times \left(\frac{e^5}{e_0^5}\right) \quad [2]$$

The choice of initial void ratio (e_0) should be somewhere between initial void ratio and post-sedimentation void ratio. The assumption of zero effective stress allows hydraulic conductivity to be calculated:

$$k_{\text{measured at } e_0} = \frac{(1+e_0)v_s}{SG-1} \quad [3]$$

Where SG is specific gravity, and v_s is the velocity of water-tailing interface. To estimate hydraulic conductivity for pilot data, the initial solid content of 41% was chosen and permeability function was obtained as:

$$k_1 = 7.6\,E-9 \times e^5 \left(\frac{m}{s}\right) \quad [4]$$

4.1.2 Method2: Estimation from density profile

In this method, Darcian flow is assumed with solids moving relative to the water:

$$-\frac{e}{1+e}(v_f - v_s) = k\frac{1}{\rho_f g}\frac{\partial u_e}{\partial x} \quad [5]$$

Where v_s and v_f are velocity of solids and fluid respectively. Material coordinates 0.1, 0.2, …, 0.9 are defined as corresponding to 10%, 20%, … and 90% of the solids, beneath the surface and solids velocity is calculated from the height of these coordinates in consecutive density profiles. Subsequently, the solids velocity is approximated by a central difference approximation (Bartholomeeusen, et al, 2002).

For pilot study, using profile density and excess pore water pressure observed in different depths of tailings, this method was used, and Eq (6) shows the obtained function for permeability.

$$k_2 = 9\,E-10 \times e^7 \left(\frac{m}{s}\right) \quad [6]$$

4.1.3 Method3: Robust back-calculation of k-e from settlement data

Qi and Simms (2019) have developed a series of methods based on innate characteristics of large strain consolidation predictions, to estimate the hydraulic conductivity function from the settlement data. Using their Method C, the third estimate of hydraulic conductivity is:

$$k_3 = 2.2E-10 \times e^8 \left(\frac{m}{s}\right) \quad [7]$$

4.2 Compressibility function

As with the permeability, the observed data collected in pilot study, were used to determine the compressibility relationship. In-situ data is shown in Figure 1. In general, the apparent compressibility function shifts downwards over time. Therefore, two compressibility functions were adopted to run the LSC model: One equation obtained from fitting the monitoring data measured at the last year (Sept 2018):

$$e = 2.019\,\sigma'^{-0.087} \quad [9]$$

While the other, was obtained from measured data from the first years of deposition:

$$e = 3.8\,\sigma'^{-0.238} \quad [10]$$

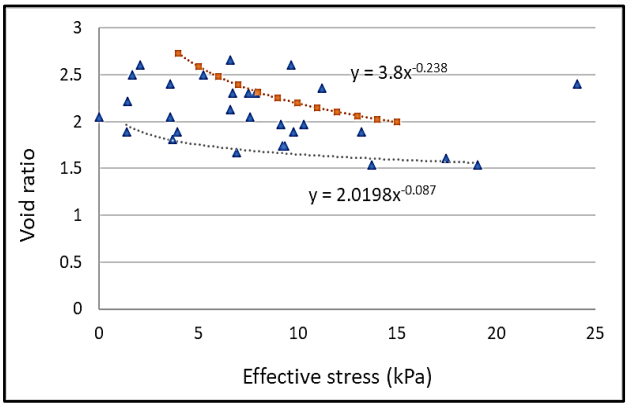

Figure 1. Compressibility functions obtained from pilot data

5 MODELLING WITHOUT CREEP

In the pilot test, deposition of the tailings occurred over 15 days. A no flux boundary is imposed at the bottom, and the accumulated water at the top due to self-weight is not removed, so condition for entire time is considered saturated. Large strain consolidation simulations were performed using a matrix of two compressibility functions and the three permeability functions. Table 1 shows the input parameters used for numerical analysis.

Table 1. Input parameters for numerical analysis-pilot study

Number of depositions	5
Thickness of each deposition (m)	2.76
Time interval between each pour (day)	3
Initial void ratio	4.67
Specific gravity	2.22
Number of nodes	50
Time increments for simulation (s)	5
Run time (days)	1100

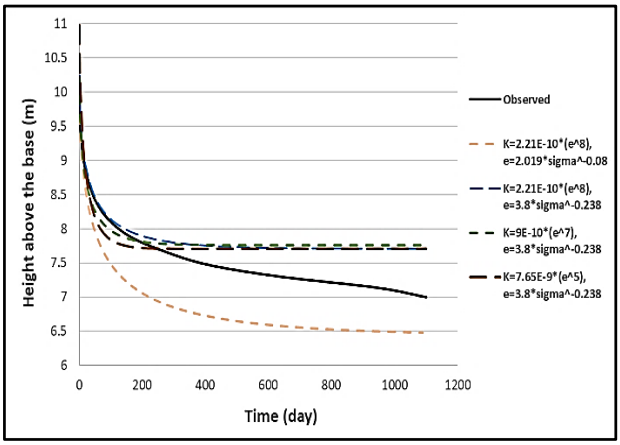

Figure 2. Large Strain Consolidation (LSC) results–settlement

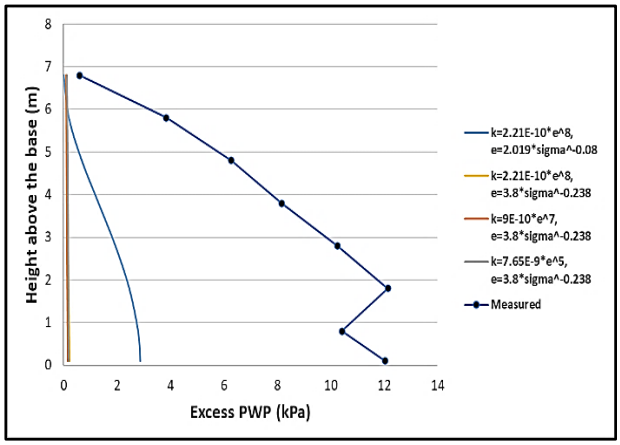

Figure 3. LSC results– excess PWP

The results of LSC simulations are shown in Figure 2 for settlement and in Figure 3 for excess pore water pressure. Generally, the results are relatively insensitive in terms of three k-e functions, but large in terms of the compressibility functions. Additionally, while the settlement predictions bracketed the observed data, all the model runs overestimated dissipation of pore-water pressure. Also, the measured settlement curve is not flat at the end of the simulated period, unlike the model results. This analysis suggests that the compressibility curve is continuing to shift.

6 ELASTO-VISCO-PLASTIC (EVP) MODELING

To incorporate the effect of creep into large strain consolidation, the Yin & Graham and Vermeer models are employed.

6.1 Yin and Graham Model

The incremental strain rate comprises of two components in Y&G model: (1) elastic strain rate that induced by effective stress change, also known as the instantaneous strain, (2) the visco-plastic strain rate, which depends on the current strain and stress state, and is evaluated based on equivalent time concepts. The original EVP model was formulated for one dimensional small strain condition; therefore, it was reformulated to a general effective stress-void ratio relationship in order to describe the large strain consolidation of loose tailings deposit as follows (Eq [11]):

$$\dot{e} = -\frac{\kappa}{\sigma'_z}\dot{\sigma}'_z - \frac{\psi}{t_0}\exp\left[\frac{e-e_0}{\psi}\right]\left(\frac{\sigma'_z}{\sigma'_{zo}}\right)^{\frac{\lambda}{\psi}} \qquad [11]$$

Where e_0 is initial void ratio corresponding to the initial effective stress σ'_{z0}; κ is the elastic stiffness of the soil; λ elastic–plastic material parameter, chosen to closely fit the first year compressibility data; ψ creep parameter, t_0 intrinsic time parameter. The equation [11] is solved in the computational program, UNSATCON, using void ratio as the independent variable.

The same scenario of depositions, that used for LSC were applied for EVP modeling, except the elasto-plastic parameters were chosen to mimic the first-year compressibility data. The adopted constitutive parameters for Y&G are shown in Figure 2.

Table 2. Input parameters for EVP modeling (Y&G)

Lambda (λ)	0.3
Kappa (κ)	0.07
Pre-consolidation stress (σ'_p)	0.2
t_0 (s)	1
Creep parameter (ψ)	0.01,0.03,0.06
Hydraulic conductivity (m/s)	Varied

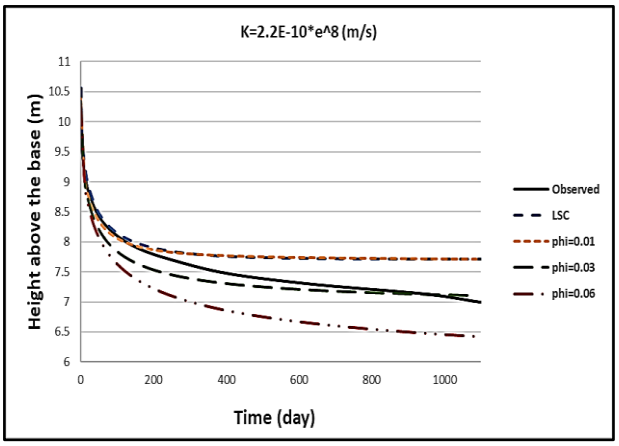

Figure 4. Creep–LSC results of Y&G model– settlement (using K=2.2E-10*e^8 (m/s))

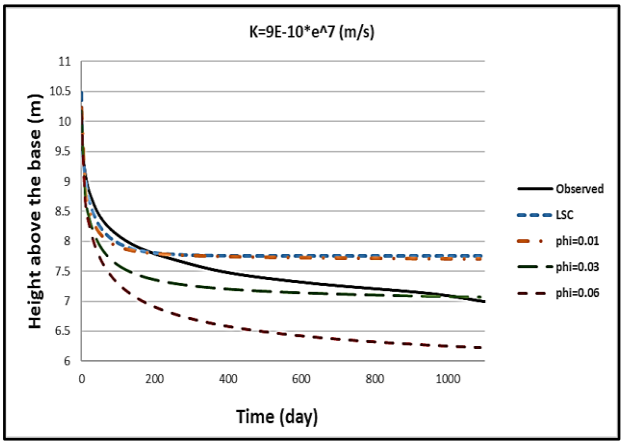

Figure 5. Creep–LSC results of Y&G model– settlement (using K=9E-10*e^7 (m/s))

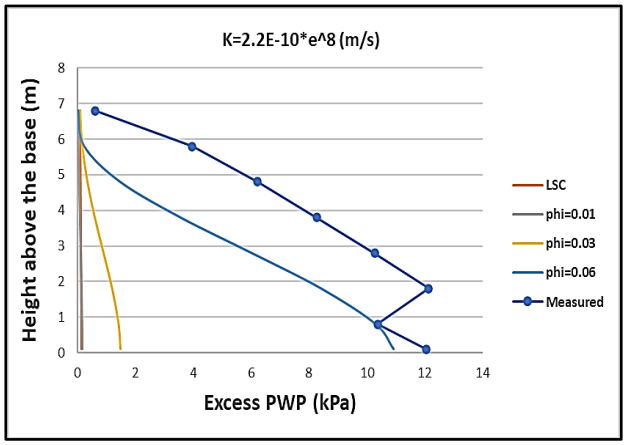

Figure 6. Creep–LSC results of Y&G model– excess PWP (using K=2.2E-10*e^8 (m/s))

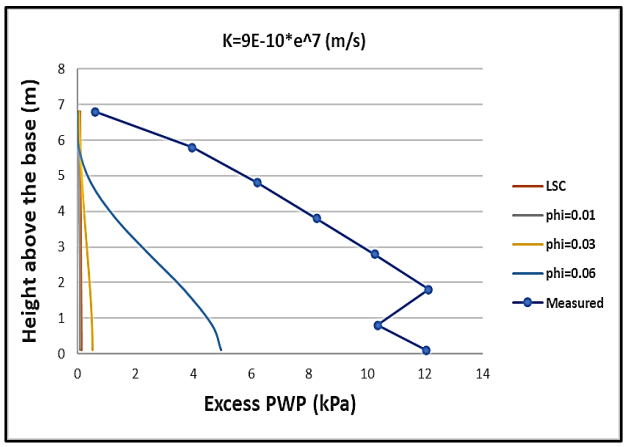

Figure 7. Creep–LSC results of Y&G model– excess PWP (using k=9E-10*e^7 (m/s))

Figures 4 and 5 compare the predicted heights using two different permeability functions vs. time curve using LSC model and Y&G model with difference creep parameters in natural time scales. Figures 6 and 7 show the simulated results of excess PWP after 1100 days using LSC and Y&G with different creep parameter. Higher values of the creep parameter mean higher creep strain rate with respect to time, the corresponding settlement is predicted to be larger than those predicted using lower creep parameter. When creep parameter is 0.01, the deposits stops settling, as the excess pore water pressure approaches zero, this observation is very close to that predicted using the conventional analysis. For the other cases with creep parameter of 0.03 and 0.06, the predicted height decreases continuously over time due to creep of material. Similarly, the excess PWP remains higher for the higher values of creep parameter. A better agreement can be achieved by increasing the creep parameter to either 0.03 (better settlement prediction) or 0.06 (overestimate of settlement, closer predicted of PWP).

6.2 Vermeer Model

In this model, as classical elasto-plasticity, the usual decomposition of total strains comprises of elastic and inelastic components that is assumed to be purely viscous. The elastic component is directly observed in fast unloading and recompression, whereas the inelastic component of strain is irreversible and time dependent. Briefly, in Vermeer model, there are 4 basics constitutive equations as described below (Leoni et al. 2008):

$$\dot{e} = \dot{e}^{e} + \dot{e}^{c} \qquad [12]$$

Where e is the void ratio; a dot over a symbol implies differentiation with respect to time; and superscripts e and c refer to the elastic and creep components, respectively. The elastic change of void ratio is formulated as:

$$\dot{e}^{e} = \frac{C_s}{\ln 10}\frac{\dot{\sigma}'}{\sigma'} \qquad [13]$$

Where σ' is the effective stress and C_s is the swelling index. The second deformation type is due to the viscous behavior of the material, which is modelled by the power law as shown in Eq (14):

$$\dot{e}^{c} = -\frac{C_a}{\tau \ln 10}\left(\frac{\sigma'}{\sigma'_p}\right)^{\beta} \quad \text{with} \quad \beta = \frac{C_c - C_s}{C_\alpha} \qquad [14]$$

Where C_α is the well-known secondary compression index, C_c is the compression index, β is the creep exponent, and τ is reference time. According to this equation, the creep rate is defined by the distance between current effective stress and current yielding. An important soil characteristic, as observed for states of normal consolidation, concerns the normal consolidation line. On this line the pre-consolidation stress σ'_p increases during creep according to the differential Eq [15]:

$$\frac{\dot{\sigma}'_p}{\sigma'_p} = -\frac{\ln 10}{C_c - C_s}\dot{e}^{c} \qquad [15]$$

Combining equations [12] and [13] gives:

$$\dot{e} = -\frac{C_s}{\ln 10}\frac{\dot{\sigma}'}{\sigma'} - \frac{C_\alpha}{\tau \ln 10}\left(\frac{\sigma'}{\sigma'_p}\right)^{\beta} \qquad [16]$$

The equations [15] and [16] were solved using fully implicit algorithm and implemented in UNSATCON. Table 3 shows the required constitutive parameters for Vermeer model, which were obtained using calibration exercise, and similar numerical parameters that used for Y&G model as Table 2 has been used for Vermeer modeling. To evaluate the results of EVP modeling, some parameters including, excess pore water pressure in different depths of deposition, and settlement over the time were compared with the observed data. To investigate any difference between two EVP models, Y&G and Vermeer models, in Figures 8 and 9 show the results of EVP simulations using Vermeer model that were compared with the results obtained from Y&G.

Table 3. Input parameters for EVP modeling (Vermeer)

Lambda (λ)	0.3
Kappa (κ)	0.07
τ (s)	3.14E+4
Creep parameter (ψ)	0.04,0.06
Hydraulic conductivity (m/s)	$K=2.2E-10*(e^{8})$

Figure 8 compares the predicted Height vs. time curve using Y&G model and Vermeer model with difference creep parameters in natural time scales. Higher values of the creep parameter results in higher creep strain rate with respect to time, the corresponding settlement is predicted to be larger than those predicted using lower creep parameter.

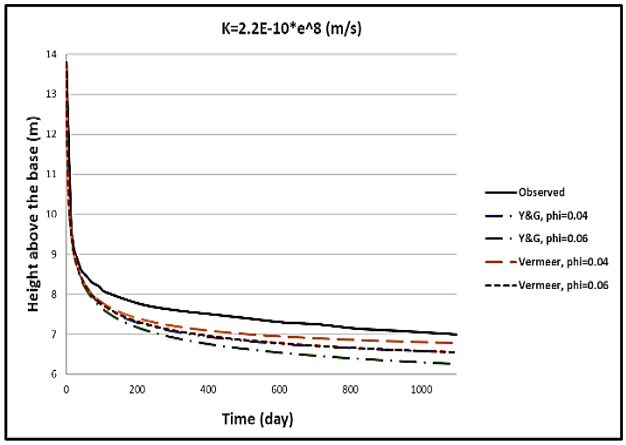

Figure 8. Creep–consolidation results for phi=0.04 and phi=0.06– settlement

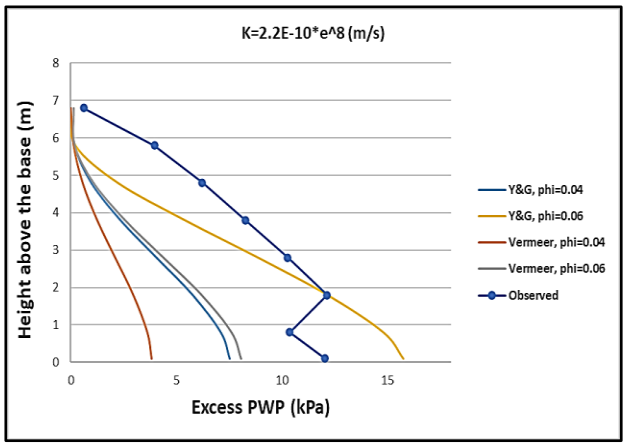

Figure 9. Creep–consolidation results for phi=0.04 and phi=0.06– excess PWP

Figure 9 shows that excess PWP show similar patterns for both models. For both models, a larger creep parameter predicts greater excess PWP but also larger settlement at a given time. Both models will either overpredict settlement for a good fit to the PWP, or underpredict excess PWP for a good fit to the observed data, depending on the creep parameter. However, choosing an intermediate creep parameter will give an improved fit to both the settlement data and the PWP data than the consolidation only model.

7 ANALYSIS OF HYPOTHETICAL CASES

To provide a range of plausible predictions for a hypothetical design case, two parameter groups that gave reasonable predictions to both the PWP and settlement pilot data were chosen, which are shown in Table 4. In this section, the Y&G model was selected for creep–consolidation modeling. The hypothetical simulation is the deposition of 10 m of fFFT every year for 5 years, and the models are run for an additional 20 years. Additional details on the hypothetical case are shown in Table 5.

Table 4. Input parameters for hypothetical cases

Case 1, Creep-consolidation	
Lambda (λ)	0.3
Kappa (κ)	0.07
Pre-consolidation stress (σ'_p)	0.2
T0(s)	1
Creep parameter (ψ)	0.03
Hydraulic conductivity (m/s)	$K=2.2E-10*(e^{8})$
Case 2, Creep-consolidation	
Lambda (λ)	0.59
Kappa (κ)	0.07
Pre-consolidation stress (σ'_p)	0.2
T0(s)	1
Creep parameter (ψ)	0.06
Hydraulic conductivity (m/s)	$K=9E-10*(e^{7})$
Case 1, Large strain consolidation	
Compressibility function	$e=3.8*(\sigma'^{-0.238})$
Hydraulic conductivity (m/s)	$K=2.2E-10*(e^{8})$
Case 2, Large strain consolidation	
Compressibility function	$e=3.8*(\sigma'^{-0.238})$
Hydraulic conductivity (m/s)	$K=9E-10*(e^{7})$

Table 5. Input parameters for numerical analysis-hypothetical cases

Number of depositions	5
Thickness of each deposition (m)	10
Time interval between each pour (day)	365
Initial void ratio	4.67
Specific gravity	2.22
Number of nodes	50
Time increments for simulation (s)	5
Run time (days)	7300

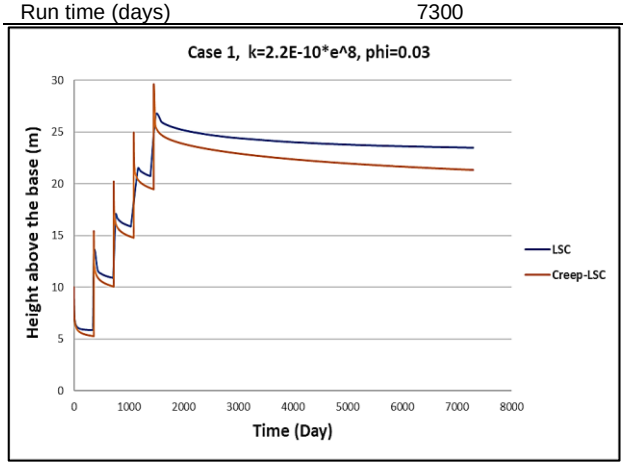

Figure 10. Settlement results– case 1

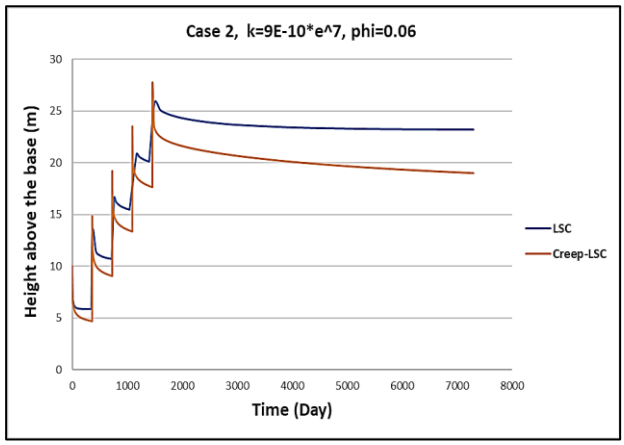

Figure 11. Settlement results– case 2

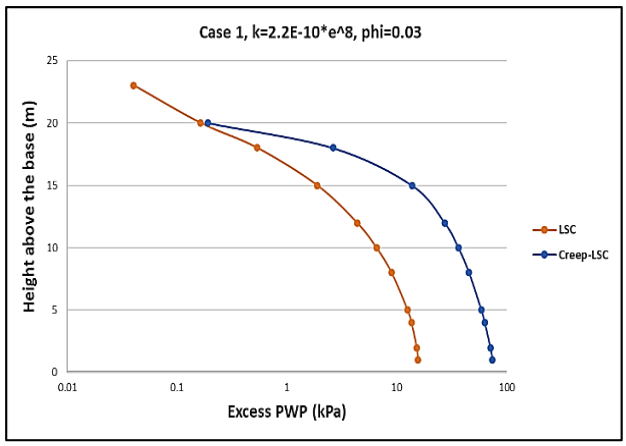

Figure 12. Excess PWP results– case 1

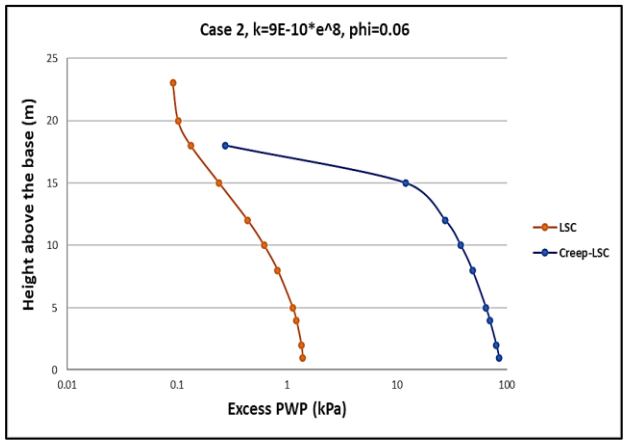

Figure 13. Excess PWP results– case 2

Figures 10 and 11 compare the predicted settlement using creep-LSC model and LSC model in natural time scales. The results for case 1 indicated that final height obtained from creep-LSC is 21.3 m while this value for LSC modeling would be 23.5 m. In Figure 11, case 2, the hydraulic conductivity is relatively higher than the hydraulic conductivity that was used for case 1, so the rate of settlement is faster while the final settlement obtained for LSC is almost the same (23.2 m) due to similar compressibility function used for simulations. Higher value of the creep parameter was resulted in higher creep strain rate with respect to time, so the corresponding settlement for case 2 was predicted as 19.0 m which is larger than what predicted using lower creep parameter (0.03) in case 1. The results for excess PWP were also represented in Figure 12 and 13. As it was observed, considering creep could results in increasing the excess PWP compared to the results from LSC. For both cases, the modeled excess PWP from LSC simulations are relatively lower compared to the excess PWP obtained from creep-consolidation. However, in case 2 compared to case 1, due to higher permeability function, almost all excess PWP using LSC were dissipated that indicated the end of primary consolidation after 20 years.

Thus, at a given time, settlement predictions between all 4 cases are relatively small, while the discrepancy in excess PWP are large. The creep models predict ongoing settlement at a logarithmically decreasing rate; For the two cases, this means about a meter of settlement between 0 to 50 years, and other meter of settlement between 50 to 100 years. However, it is the nature of these creep models that creep is unending, which is not likely true. Creep may be also overtaken by the ageing phenomena.

8 CONCLUSIONS

The large strain consolidation – creep modeling was conducted for fFFT deposit in a pilot study using two different EVP constitutive models embedded in the UNSATCON software. Numerical simulations using three different permeability and two compressibility functions obtained from field data show that (1) LSC is not able to predict the actual dewatering behaviors in oil sands tailings, as the excess PWP has been totally dissipated after approximately 300 days while continuous consolidation/settlement can be observed in the field. (2) incorporation of creep into large strain consolidation improved fits to settlement and excess PWP, in compared with the large strain consolidation only results, however the agreement still is not perfect. (3) numerical results of Vermeer model and Y&G model showed that both models predict qualitatively similar results (4) the results for two hypothetical cases indicated the significant differences that can be caused by incorporation creep into LSC for full scale deposits in terms of predicted settlement and excess PWP. It should be mentioned that these EVP modeling have several limitations, including the necessity for obtaining parameters to describe the creep behavior which are not simple to determine. Moreover, other time-dependent effects such as aging(structuration) must be considered and incorporated into large strain consolidation that is ongoing by authors.

ACKNOWLEDGEMENTS

This work is funded through a joint NSERC-COSIA Collaborative Research Development Grant awarded to

the last author. Logistical support and data sharing by COSIA member companies is gratefully acknowledged.

9 REFERENCES

Babaoglu, Y. and Simms, P. (2018). Estimating saturated hydraulic conductivity from compression curve for fluid fine tailings. Proceedings of GeoEdmonton, 71st Canadian Geotechnical Conference, Edmonton.

Bartholomeeusen, G., et al. "Sidere: numerical prediction of large-strain consolidation." Géotechnique 52.9 (2002): 639-648.

Gibson, R. E., Schiffman, R. L., & Cargill, K. W. (1981). The theory of one-dimensional consolidation of saturated clays. II. Finite nonlinear consolidation of thick homogeneous layers. *Canadian Geotechnical Journal*, *18*(2), 280-293.

Jeeravipoolvarn, S., Scott, J. D., & Chalaturnyk, R. J. (2009). 10 m standpipe tests on oil sands tailings: long-term experimental results and prediction. Canadian geotechnical journal, 46(8), 875-888.

Leoni, M. Karstunen, M. and Vermeer, P. A. (2008), Anisotropic creep model for soft soils Canadian Geotechnical Journal, 58(3), 215–226.

Leroueil, S. (2006, May). The Isotache approach. Where are we 50 years after its development by Professor Šuklje? 2006 Prof. Šuklje's Memorial Lecture. In Proceedings of the XIII Danube-European Conference on Geotechnical Engineering, Ljubljana, Slovenia (Vol. 2, pp. 55-88).

Liingaard, M., Augustesen, A. & Lade, P. V. (2004). Characterization of models for time-dependent behavior of soils. Int. J. Geomech. 4, No. 2, 157–177.

McKenna, G., Mooder, B., Burton, B. and Jamieson, A. 2016. Shear strength and density of oil sands fine tailings for reclamation to a boreal forest landscape. Proceedings of the Fifth International Oil Sands Tailings Conference (IOSTC), December 4-7, 2016, Lake Louise, Alberta.

Qi, S., Simms, P., & Vanapalli, S. (2017). Piecewise-linear formulation of coupled large-strain consolidation and unsaturated flow. I: Model development and implementation. Journal of Geotechnical and Geoenvironmental Engineering, 143(7), 04017018.

Qi, S., Simms, P., Vanapalli, S., & Daliri, F. 2016. A large strain consolidation-unsaturated flow model for tailings analysis: multilayers. *Proceedings of GeoVancouver 2016,* 69th Canadian Geotechnical Conference, electronic proceedings.

Qi, S., Simms, P., Vanapalli, S., & Soleimani, S. (2017). Piecewise-Linear Formulation of Coupled Large-Strain Consolidation and Unsaturated Flow. II: Testing and Performance. Journal of Geotechnical and Geoenvironmental Engineering, 143(7), 04017019.

Salam, A, Simms, P, Ormeci, B. 2017. Investigation of creep in polymer amended oil sands tailings. Submitted to 2017 Canadian Geotechnical Conference.

Sills, G. (1998). Development of structure in sedimenting soils. PHILOSOPHICAL TRANSACTIONS-ROYAL SOCIETY OF LONDON SERIES A MATHEMATICAL PHYSICAL AND ENGINEERING SCIENCES, 2515-2534.

Vermeer, P. A. & Neher, H. P. (1999). A soft soil model that accounts for creep. Proceedings of the international symposium 'Beyond 2000 in Computational Geotechnics', Amsterdam, pp. 249–261.

Yin, J.-H. & Graham J. (1999). Elastic viscoplastic modelling of the time dependent stress–strain behaviour of soils. Can. Geotech. J. 36, No. 4, 736–745.